Current Biology, Volume *30*

Supplemental Information

Genomic Adaptations and Evolutionary History of the Extinct Scimitar-Toothed Cat, *Homotherium latidens*

Ross Barnett, Michael V. Westbury, Marcela Sandoval-Velasco, Filipe Garrett Vieira, Sungwon Jeon, Grant Zazula, Michael D. Martin, Simon Y.W. Ho, Niklas Mather, Shyam Gopalakrishnan, Jazmín Ramos-Madrigal, Marc de Manuel, M. Lisandra Zepeda-Mendoza, Agostinho Antunes, Aldo Carmona Baez, Binia De Cahsan, Greger Larson, Stephen J. O'Brien, Eduardo Eizirik, Warren E. Johnson, Klaus-Peter Koepfli, Andreas Wilting, Jörns Fickel, Love Dalén, Eline D. Lorenzen, Tomas Marques-Bonet, Anders J. Hansen, Guojie Zhang, Jong Bhak, Nobuyuki Yamaguchi, and M. Thomas P. Gilbert

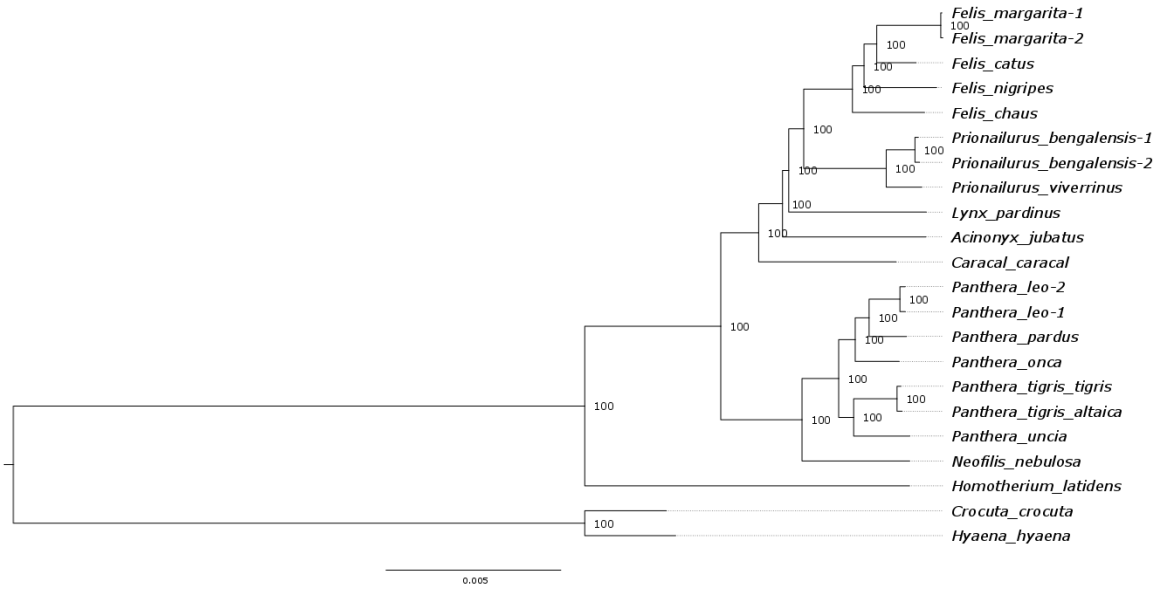

Figure S1: Maximum likelihood phylogenetic tree constructed using a concatenated supermatrix of 29,216,712 bp. Related to Figure 1 and STAR methods phylogenetic analyses. Numbers at the nodes show bootstrap support values. Branch lengths show the average number of substitutions per site.

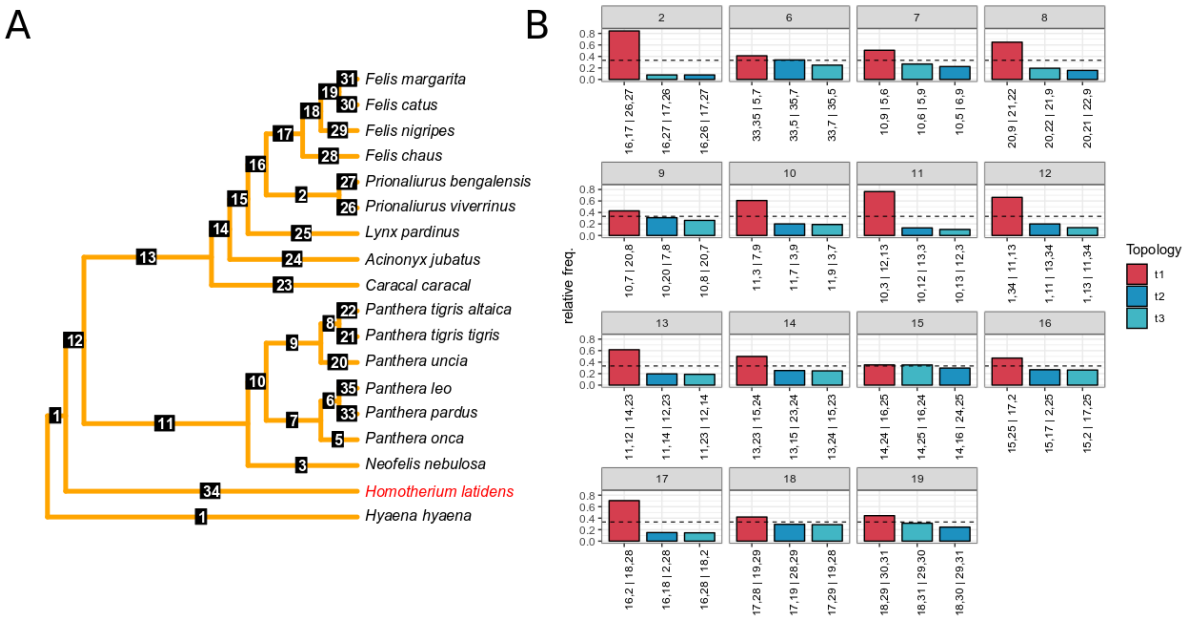

Figure S2. Phylogenetic analyses for tree topology discordances in the Felidae. Related to Figure 1 and STAR methods phylogenetic analyses. A) Species tree under the multispecies coalescent inferred from the maximum-likelihood gene trees. Branches have been numerically labelled for easy identification. **B)** Relative frequencies of the three possible bipartitions (possible arrangements of a quartet on an unrooted tree) induced by each internal branch of the estimated species tree. X axis numbers correspond to branch labels in A written in a quartet fashion based on the topology ([A,B],[C,D]). Dashed lines show the threshold value of ⅓, shown theoretically to be the minimum frequency for a true bipartition. Related to Figure 1 and STAR methods phylogenetic analyses.

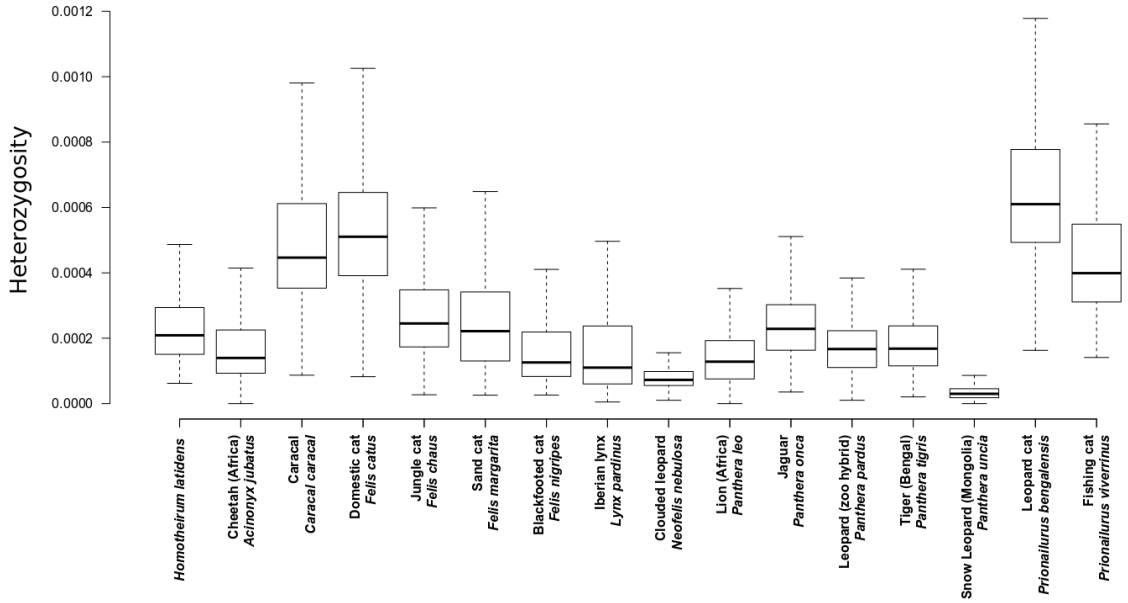

Figure S3: Exome-wide heterozygosity estimates based single representatives for each species used in the current study. Related to Figure 3 and STAR methods genetic diversity. Variance was estimated by independently calculating the average heterozygosity in non-overlapping windows of 200kb of covered bases.

Node	Node age (Ma)[a]				
	Correlated-rates model	**Independent-rates model**	**Low rate prior: Gamma(1,50)**	**High rate prior: Gamma(1,2)**	**Prior (no data)**
Root	32.8	32.3	33.0	32.8	32.4
Homotherium-sister	22.5	16.7	22.6	22.6	30.3
Pantherinae-Felinae	14.1	10.2	14.1	14.1	28.3
Neofelis-Panthera	8.3	5.5	8.3	8.3	23.3
Panthera	5.4	3.4	5.4	5.4	17.9
Caracal-sister	11.3	8.3	11.3	11.3	24.9
Acinonyx-sister	9.7	7.1	9.6	9.7	21.6
Lynx-sister	9.2	6.7	9.2	9.2	17.2
Prionailurus-Felis	8.2	6.0	8.1	8.2	12.7
Felis	5.0	3.8	5.0	5.0	9.2

Table S1 - Ages of key nodes in the phylogeny, estimated under a range of settings. Related to Figure 1 and STAR methods phylogenomic dating. The time-tree in Figure 1 is based on the correlated-rates model. [a]Correlated-rates model: Rates are assumed to be correlated between neighbouring branches in the phylogeny. Independent-rates model: Rates are assumed to be identically and independently distributed across branches in the phylogeny. Low rate prior: Gamma(1,50) prior for the rate, with a prior mean of 0.0002 substitutions/site/Myr. High rate prior: Gamma(1,2) prior for the rate, with a prior mean of 0.005 substitutions/site/Myr. Prior (no data): Analysis run without sequence data, such that the node ages are sampled from the joint prior.

GeneName	OneRatio	FreeRatio	Biological role	Functional role
AGBL5	0.97893	3.7966	vision sensitivity to diurnal light and circadian rhythms	vision
AK3	1	2.5265	endurance	mitochondria respiration
B3GALNT2	1	4.501	vision sensitivity to diurnal light and circadian rhythms	vision
C13orf30	1	2.3383	unknown	unknown
CAPNS2	1	2.8782	vision sensitivity to diurnal light and circadian rhythms	vision
ECSCR	1	3.4687	endurance	angiogenesis
F5	0.0001	3.3227	endurance	circulatory system
GCM1	1	2.0195	reproduction	placenta
GOLT1A	1	4.4857	cell function	Golgi
GPRC5A	1	2.7265	immunity	cancer
HMGB2	1	2.127	immunity	fecundity
IQCF5	0.64872	2.3567	unknown	unknown
ISCU	1	2.3704	endurance	mitochondria respiration
LAGE3	1	2.449	cell function	apoptosis
MIS18A	1	3.7168	cell function	mitosis
MMP12	1	2.2541	endurance	respiratory/circulatory system
NTF3	1	4.3076	socialisation	nervous system
OR11A1	0.83912	3.7452	olfaction	olfaction
Per1	0.02951	2.0949	vision sensitivity to diurnal light and circadian rhythms	circadian clock
PGD	1	2.8531	bone mineralization	bone mineralization
Rplp1	0.0001	3.1993	ribosome	protein synthesis
Rps13	1	2.4235	ribosome	protein synthesis
SCTR	1	2.8874	socialisation	social behaviour
SDPR	0.98745	2.3358	endurance	angiogenesis
SFPQ	1	2.4583	vision sensitivity to diurnal light and circadian rhythms	circadian clock

SLC1A7	1	2.1567	vision sensitivity to diurnal light and circadian rhythms	vision
SPACA3	0.0001	3.0126	reproduction	sperm
STAP1	0.99486	2.2366	cell function	docking protein
SURF1	1	2.1957	endurance	mitochondria respiration
TAF8	0.97884	2.9587	endurance	adipogenesis
TMEM45A	0.99662	4.899	endurance	hypoxia
unknown	0.99995	2.1152	unknown	unknown

Table S3: 31 genes under positive selection in the *Homotherium* genome with high values (free-ratio > 2) detected using one-ratio/free-ratio models and their respective hypothetical biological and functional roles. Related to Figure 2 and STAR methods and tests of positive selection.